



CHALMERS

Chalmers Publication Library

Comparison of 128-SP-QAM with PM-16-QAM

This document has been downloaded from Chalmers Publication Library (CPL). It is the author's version of a work that was accepted for publication in:

Optics Express (ISSN: 1094-4087)

Citation for the published paper:

Sjödin, M. ; Johannisson, P. ; Li, J. (2012) "Comparison of 128-SP-QAM with PM-16-QAM". Optics Express, vol. 20(8), pp. 8356-8366.

<http://dx.doi.org/10.1364/OE.20.008356>

Downloaded from: <http://publications.lib.chalmers.se/publication/156096>

Notice: Changes introduced as a result of publishing processes such as copy-editing and formatting may not be reflected in this document. For a definitive version of this work, please refer to the published source. Please note that access to the published version might require a subscription.

Chalmers Publication Library (CPL) offers the possibility of retrieving research publications produced at Chalmers University of Technology. It covers all types of publications: articles, dissertations, licentiate theses, masters theses, conference papers, reports etc. Since 2006 it is the official tool for Chalmers official publication statistics. To ensure that Chalmers research results are disseminated as widely as possible, an Open Access Policy has been adopted. The CPL service is administrated and maintained by Chalmers Library.

(article starts on next page)

Comparison of 128-SP-QAM with PM-16-QAM

Martin Sjödin,^{1,*} Pontus Johannisson,¹ Jianqiang Li,¹ Erik Agrell,²
Peter A. Andrekson,¹ and Magnus Karlsson,¹

¹Department of Microtechnology and Nanoscience, Chalmers University of Technology, Kemivägen 9, SE-41296, Gothenburg, Sweden

²Department of Signals and Systems, Chalmers University of Technology, Hörsalsvägen 9-11, SE-41296, Gothenburg, Sweden

*martin.sjodin@chalmers.se

Abstract: In this paper we investigate an interesting modulation format for fiber optic communications, set-partitioning 128 polarization-multiplexed 16-QAM (128-SP-QAM), which consists of the symbols with even parity from the symbol alphabet of polarization-multiplexed 16-QAM (PM-16-QAM). We compare 128-SP-QAM and PM-16-QAM using numerical simulations in long-haul transmission scenarios at bit rates of 112 Gbit/s and 224 Gbit/s, and at the same symbol rates (14 and 28 Gbaud). The transmission link is made up of standard single-mode fiber with 60, 80 or 100 km amplifier spacing and both single channel and WDM transmission (25- and 50 GHz-spaced) is investigated. The results show that 128-SP-QAM achieves more than 40% increase in transmission reach compared to PM-16-QAM at the same data rate for all cases studied for a bit error rate of 10^{-3} . In addition, we find that in single channel transmission there is, as expected, an advantage in terms of transmission distance when using a data rate of 112 Gbit/s as compared to 224 Gbit/s. However, when comparing the two different WDM systems with the same aggregate data rates, the reach is similar due to the smaller impact of nonlinear crosstalk between the WDM channels in the systems with 50 GHz spacing. We also discuss decoding and phase estimation of 128-SP-QAM and implement differential coding, which avoids error bursts due to cycle slips in the phase estimation. Simulations including laser phase noise show that the phase noise tolerance is similar for the two formats, with 0.5 dB OSNR penalty compared to the case with zero phase noise for a laser linewidth to symbol rate ratio of 10^{-4} .

©2012 Optical Society of America

OCIS codes: (060.0060) Fiber optics and optical communications; (060.4080) Modulation; (060.1660) Coherent communications.

References and links

1. D.-S. Ly-Gagnon, S. Tsukamoto, K. Katoh, and K. Kikuchi, "Coherent detection of optical quadrature phase-shift keying signals with carrier phase estimation," *J. Lightwave Technol.* **24**(1), 12–21 (2006).
2. H. Sun, K. T. Wu, and K. Roberts, "Real-time measurements of a 40 Gb/s coherent system," *Opt. Express* **16**(2), 873–879 (2008).
3. J.-X. Cai, Y. Cai, C. R. Davidson, D. G. Foursa, A. J. Lucero, O. V. Sinkin, W. W. Patterson, A. N. Pilipetskii, G. M. Mohs, and N. S. Bergano, "Transmission of 96x100-Gb/s bandwidth-constrained PDM-RZ-QPSK channels with 300% spectral efficiency over 10610 km and 400% spectral efficiency over 4370 km," *J. Lightwave Technol.* **29**(4), 491–498 (2011).
4. P. J. Winzer, A. H. Gnauck, C. R. Doerr, M. Magarini, and L. L. Buhl, "Spectrally efficient long-haul optical networking using 112-Gb/s polarization-multiplexed 16-QAM," *J. Lightwave Technol.* **28**(4), 547–556 (2010).
5. A. Sano, H. Masuda, T. Kobayashi, M. Fujiwara, K. Horikoshi, E. Yoshida, Y. Miyamoto, M. Matsui, M. Mizoguchi, H. Yamazaki, Y. Sakamaki, and H. Ishii, "Ultra-high capacity WDM transmission using spectrally-efficient PDM 16-QAM modulation and C- and extended L-band wideband optical amplification," *J. Lightwave Technol.* **29**(4), 578–586 (2011).
6. M. Karlsson and E. Agrell, "Which is the most power-efficient modulation format in optical links?" *Opt. Express* **17**(13), 10814–10819 (2009).
7. E. Agrell and M. Karlsson, "Power-efficient modulation formats in coherent transmission systems," *J. Lightwave Technol.* **27**(22), 5115–5126 (2009).

8. X. Liu, T. H. Wood, R. W. Tkach and S. Chandrasekhar "Demonstration of record sensitivity in an optically pre-amplified receiver by combining PDM-QPSK and 16-PPM with pilot-assisted digital coherent detection," in *National Fiber Optic Engineers Conference*, OSA Technical Digest (CD) (Optical Society of America, 2011), paper PDPB1.
9. H. Bülow, "Polarization QAM modulation (POLQAM) for coherent detection schemes," in *Optical Fiber Communication Conference*, OSA Technical Digest (CD) (Optical Society of America, 2009), paper OWG2.
10. L. D. Coelho and N. Hanik, "Global optimization of fiber-optic communication systems using four-dimensional modulation formats," in *37th European Conference and Exposition on Optical Communications*, OSA Technical Digest (CD) (Optical Society of America, 2011), paper Mo.2.B.4. .
11. G. Ungerboeck, "Channel coding with multilevel/phase signals," *IEEE Trans. Inf. Theory* **28**(1), 55–67 (1982).
12. P. Poggiolini, G. Bosco, A. Carena, V. Curri, and F. Forghieri, "Performance evaluation of coherent WDM PS-QPSK (HEXA) accounting for nonlinear fiber propagation effects," *Opt. Express* **18**(11), 11360–11371 (2010).
13. M. Karlsson and E. Agrell, "Spectrally efficient four-dimensional modulation," in *Optical Fiber Communication Conference*, OSA Technical Digest (Optical Society of America, 2012), paper OTu2C.1
14. J. H. Conway and N. J. A. Sloane, "Fast quantizing and decoding algorithms for lattice quantizers and codes," *IEEE Trans. Inf. Theory* **28**(2), 227–232 (1982).
15. T. Pfau, S. Hoffmann, and R. Noé, "Hardware-efficient coherent digital receiver concept with feedforward carrier recovery for M-QAM constellations," *J. Lightwave Technol.* **27**(8), 989–999 (2009).
16. P. Johannisson, M. Sjödin, M. Karlsson, H. Wymeersch, E. Agrell, and P. A. Andrekson, "Modified constant modulus algorithm for polarization-switched QPSK," *Opt. Express* **19**(8), 7734–7741 (2011).
17. C. Xie, "Local oscillator induced penalties in optical coherent detection systems using electronic chromatic dispersion compensation," in *Optical Fiber Communication Conference*, OSA Technical Digest (CD) (Optical Society of America, 2009), paper OMT4.
18. D. Wang and C. R. Menyuk, "Polarization evolution due to the Kerr nonlinearity and chromatic dispersion," *J. Lightwave Technol.* **17**(12), 2520–2529 (1999).
19. P. Serena, A. Vannucci, and A. Bononi, "The performance of polarization switched QPSK (PS-QPSK) in dispersion managed WDM transmissions," in *2010 36th European Conference and Exhibition on Optical Communication (ECOC)* (2010), paper Th.10.E.2.
20. P. Poggiolini, G. Bosco, A. Carena, V. Curri, V. Miot, and F. Forghieri, "Performance dependence on channel baud-rate of PM-QPSK systems over uncompensated links," *IEEE Photon. Technol. Lett.* **23**(1), 15–17 (2011).

1. Introduction

On-off keying was for a long time the dominating modulation format, as there was no strong motivation to look at more advanced options. The reason was that technologies such as the erbium-doped fiber amplifier (EDFA) and wavelength division multiplexing (WDM) enabled higher data rates by simply adding more channels in the systems. However, in many systems the C-band is now fully occupied with WDM channels and researchers are spending a lot of efforts on investigating modulation formats with higher spectral efficiency to enable even higher data rates. In addition, these modulation formats should preferably have high power efficiency and reasonable implementation complexity on both the transmitter and the receiver side.

The digital coherent receiver enables the use of modulation formats that take advantage of both quadratures and both polarization states of the electromagnetic field. Polarization-multiplexed quadrature phase-shift keying (PM-QPSK) and polarization-multiplexed rectangular 16-ary quadrature amplitude modulation (PM-16-QAM) are two good examples of such formats. PM-QPSK is at this time well investigated [1–3] and already in commercial use. It enables transmission at high spectral efficiency in long-haul systems and will probably be the dominating modulation format in long-haul transmission in the foreseeable future.

PM-16-QAM, which is a promising next step after PM-QPSK to further increase the spectral efficiency [4, 5], will most likely be used in commercial systems within a few years. Like PM-QPSK, PM-16-QAM does not fully exploit the four-dimensional (4D) signal space of the optical carrier wave, since it transmits independent constellations in each of the two orthogonal polarization states of the fiber. However, recent work has shown that more power-efficient formats, i.e. formats with larger minimum distance between different symbols at a given average power, can be found by taking all four dimensions into account when designing the constellation for a given number of levels in a modulation format, as opposed to choosing a format optimized in a two-dimensional space and transmit such constellations independently over the two polarizations. By means of sphere-packing simulations, polarization-switched QPSK was found to be the most power-efficient modulation format in fiber optic communication systems for signal spaces with up to four dimensions [6, 7]. Further gains can

be obtained by generalized pulse-position modulation [8] or by coding. Furthermore, Bülow [9] has demonstrated polarization-QAM (POL-QAM) modulation, which is an extension of PM-QPSK to six polarization states with one additional bit per two PM-QPSK symbols. The extra bit was used to implement an inner forward error correction code but may also be used for other purposes such as increasing the data rate.

Going on to more spectrally efficient 4D formats, Coelho and Hanik [10] recently introduced two additional modulation formats to the fiber optic communication research community by applying the Ungerboeck set-partitioning scheme [11], to PM-16-QAM. These formats were called set-partitioning 32 PM-16-QAM and set-partitioning 128 PM-16-QAM (128-SP-QAM). The names stem from the remaining number of symbols in the PM-16-QAM symbol alphabet after the set partitioning. Thus, in 128-SP-QAM, 50% of the symbols of PM-16-QAM have been removed, and only the symbols with an even number of “one bits”, i.e. the symbols with even parity, remain.

We here present the first detailed comparison between 128-SP-QAM and PM-16-QAM in long-haul transmission scenarios by using numerical simulations of the nonlinear Schrödinger equation. The formats are compared in both single-channel systems and in two different WDM systems, a 25 GHz-spaced system operating at 112 Gbit/s and another with 50 GHz spacing and 224 Gbit/s data rate per channel. Similarly to [12], we also look at a scenario in which a switch to a more power-efficient modulation format is made to keep a failing link in operation at the cost of a bit rate reduction, which in this case is 12.5%. This gives 128-SP-QAM 2 dB back-to-back optical signal-to-noise ratio (OSNR) advantage and around 50% increase in transmission distance at a received bit error rate (BER) of 10^{-3} after coherent detection. The formats are compared for fiber span lengths of 60, 80, and 100 km, and it is found that 128-SP-QAM allows for significantly increased transmission distances compared to PM-16-QAM in all cases.

Furthermore, we show that 128-SP-QAM can be differentially coded and that joint phase estimation for the signals from the two polarization states is not required, in spite of the fact that the modulation format is 4D. This makes the format more interesting for implementation, as higher-order QAM formats are known to be sensitive to cycle slips in the phase estimation.

The paper is organized as follows: In section 2, we describe 128-SP-QAM with non-differential and differential coding and the digital signal processing (DSP) for the format. In section 3, we present the setup for the numerical simulations, and the numerical results are presented in section 4. Finally, the conclusions are given in section 5.

2. Power efficiency and decoding of 128-SP-QAM

The power efficiency is calculated by dividing the minimum distance between symbols in the constellation with the average power [6]. For 128-SP-QAM, this gives an asymptotic power efficiency (i.e. at an arbitrarily small BER) of -1.55 dB compared to PM-QPSK and $+2.45$ dB compared to PM-16-QAM at a fix bit rate [13]. At higher BER the difference in power efficiency between the formats is smaller. For example, in [10] the simulated difference in required OSNR between 128-SP-QAM and PM-16-QAM at a BER of 10^{-3} was 1.3 dB.

2.1 Non-differential coding

128-SP-QAM with non-differential coding is generated as follows: Start from a codeword with seven information bits. Create a “parity bit” by performing an XOR operation on the information bits. The 4D symbol now contains eight bits and is part of the subset of even parity symbols in the symbol alphabet of Gray-coded PM-16-QAM.

An example of the generation of a 128-SP-QAM symbol is shown in Figs. 1(a)-(c). We have a bit sequence with an odd number of ones, 1101011. The parity bit is therefore a one, and the resulting symbols in the x- and the y-polarization states are shown in Figs. 1(b)-(c).

To decode a 128-SP-QAM symbol using non-differential coding, the scheme from [14] is used. In words, it can be described:

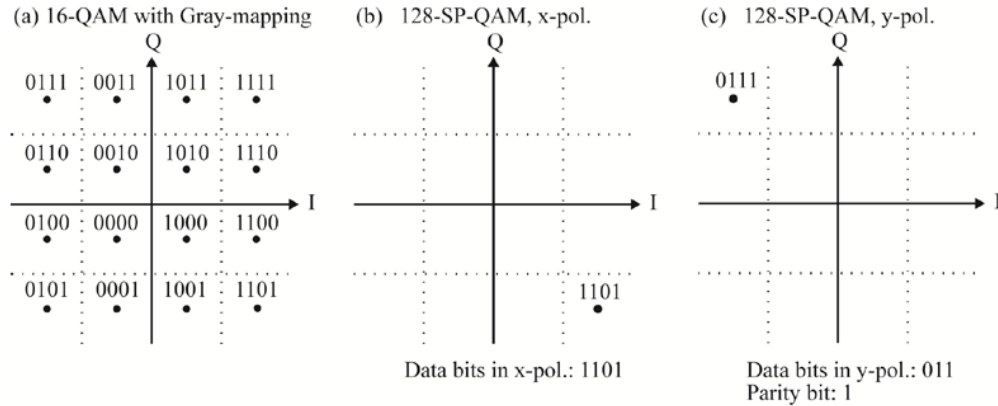


Fig. 1. (a) Gray-coded 16-QAM in one polarization. (b)-(c) The example 128-SP-QAM symbol with the bit sequence 1101011 in the x- and the y-polarizations, respectively.

1. Find two 16-QAM symbols independently by using the signals in the two polarizations. Decode the Gray-coded 16-QAM symbols to obtain eight bits.
2. Manipulate the detected 4D signal by moving it over the closest decision threshold [14]. (This inverts the most uncertain bit, i.e. the only one of the eight bits affected by this operation.) Decode the 4D signal as above.
3. Check the parity of the two bit sequences derived from step 1 and step 2 (which will be different). Keep only the one with even parity. Discard the parity bit.

We note here that steps 1 and 2 can be carried out in parallel.

2.2 Differential coding

The bit-to-symbol mapping for 16-QAM with differential coding [15] is shown in Fig. 2. Two bits are coded in the transitions between the quadrants in the complex plane, while the remaining two bits are Gray-coded within each quadrant. Differential coding gives an OSNR penalty (0.4 dB for a BER of 10^{-3} [15]) compared to non-differential coding with Gray-coding, but has the benefit that error bursts due to cycle slips are avoided. As 16-QAM is much more sensitive than QPSK to signal distortion and laser phase noise [15], differential coding may be compulsory. We have therefore investigated the possibility of using this type of coding for 128-SP-QAM. As the two polarizations are part of a 4D signal space for this format, it is not obvious whether differential coding can be used and what the implications are. For example, PS-QPSK may be differentially coded, but a joint phase estimate is required to avoid error bursts due to cycle slips. The differential coding for 128-SP-QAM that we propose is similar as for differentially coded PM-16-QAM, but with one of the eight information bits replaced by the parity bit. We choose to use one of the Gray-coded bits in the y-polarization as the parity bit.

Looking at the differentially coded 16-QAM constellation in Fig. 2, we notice that if a symbol is mistaken for its nearest neighbor, an odd number of bit errors will occur. This leads to a parity error and the bit errors will be corrected by the decoding algorithm. A cycle slip will lead to a single symbol error but not an error burst with this type of coding.

To decode a 128-SP-QAM signal that uses differential coding we can use the algorithm described above with one modification: The symbol corresponding to the even parity bit sequence should be saved and used in the decoding of the following symbol, to avoid an error in the next differential transition.

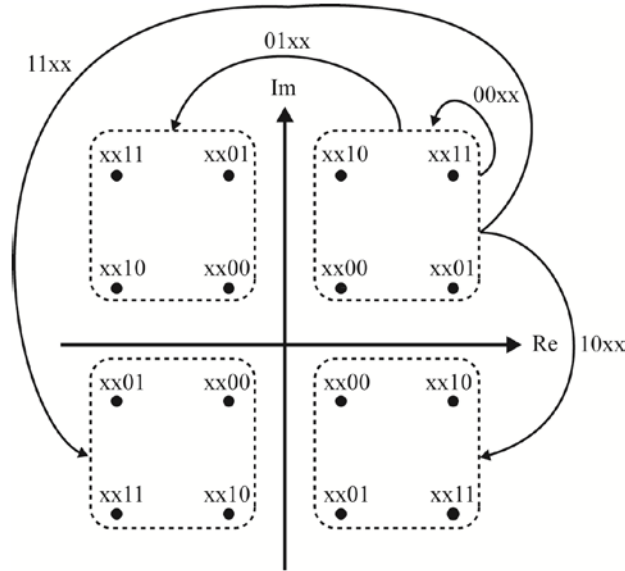


Fig. 2. 16-QAM with differential coding.

2.3 DSP for 128-SP-QAM

We have found that the DSP algorithms commonly used for PM-16-QAM can be used also for 128-SP-QAM. This is not obvious, as for example PS-QPSK, which may be described as PM-QPSK with one set partitioning, requires a different algorithm for polarization demultiplexing as compared to PM-QPSK [16]. For both formats investigated in this paper, we used CMA followed by a decision-directed least mean square (DD-LMS) algorithm [4] for polarization demultiplexing and equalization. CMA is used in the initial stage and, once sufficient pre-convergence has been achieved, a switch is made to the DD-LMS algorithm. For phase estimation we used the algorithm in [15]. As shown in section 4, the performance of the algorithms is similar for the two formats.

3. Numerical simulations

We have carried out numerical simulations of the performance of 128-SP-QAM with differential coding and compared with differentially coded PM-16-QAM. We have investigated the back-to-back performance and the impact from transmission impairments in fiber links with different span lengths. In the back-to-back case we included a comparison of the laser phase noise tolerance of the two formats, but in the transmission simulations we neglected laser phase noise. It is well known that the interaction between local oscillator phase noise and DSP-based chromatic dispersion (CD) compensation may degrade the

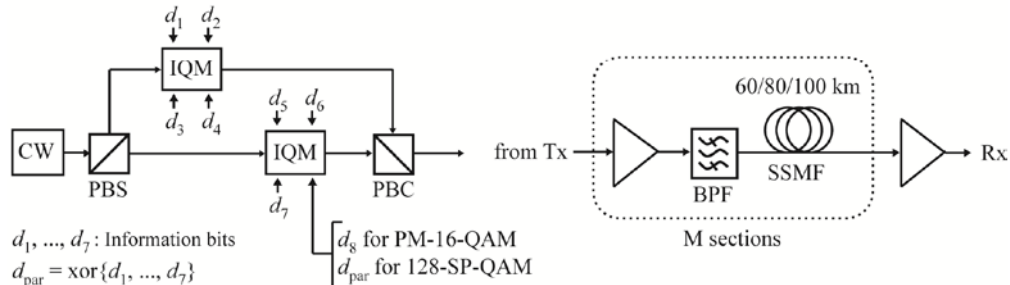


Fig. 3. (a) The transmitter used to generate 128-SP-QAM and PM-16-QAM. (b) The transmission link.

performance in long-haul transmission systems [17], especially at high data rates. However, such interaction can be made negligible by using lasers with narrow linewidths and here we choose to focus on the transmission performance of the two modulation formats.

As a model for light propagation in an optical fiber, we used the Manakov model together with attenuation [18]. This equation describes propagation in a fiber with rapidly and randomly varying birefringence, which is the case for most sufficiently long transmission fibers.

3.1 Transmitter

The transmitter setup is shown in Fig. 3(a) and is identical for both modulation formats except for the symbol rate dependent electrical filter bandwidths. The continuous wave (CW) output from a laser is split and modulated in each polarization state by an IQ-modulator (IQM) driven by four-level electrical signals, each generated by combining two binary signals with the amplitude ratio 1:2. In the case of 128-SP-QAM, one of the binary signals, d_{par} , is used to make the parity of the symbols even. For the data signals we used sequences of 2^{16} bits with random data that were different for each WDM channel. The driving signals to the modulator are bandwidth-limited by a 5th order Bessel filter (3-dB bandwidth of 0.75 times the symbol rate). Before wavelength multiplexing, each channel was filtered by a super-Gaussian filter of the second order and a 3-dB bandwidth of 22 and 44 GHz for data rates of 112 Gbit/s and 224 Gbit/s, respectively, resulting in good agreement with the measured transfer functions of commercial interleaver filters. The same type of filter was used in the receiver to demultiplex the channels.

In the simulations of linewidth tolerance, the phase noise was modeled as a Wiener process with variance $\sigma_p^2 = 2\pi\Delta\nu \cdot T$, where $\Delta\nu$ is the combined linewidth of the transmitter and LO lasers and T is the symbol period.

3.2 The link

The fiber link, shown in Fig. 3(b), consists of a number of identical sections with an EDFA followed by a span of SSMF. To investigate the impact of different span lengths, we used 60, 80, and 100 km. ASE noise from the EDFAs was added at each amplifier, as opposed to adding all the noise after transmission which is sometimes done to reduce the simulation time. The band-pass filter (BPF, 4th order super-Gaussian) after each EDFA was used to suppress ASE noise outside the signal spectra. In the single channel case, the 3-dB bandwidth was 50 GHz and 100 GHz for data rates of 112 Gbit/s and 224 Gbit/s, respectively, and in the WDM case it was wide enough to accommodate the whole WDM spectra. The BER was measured as a function of the fiber span launch power per channel and the link length. We used the following parameter values in the transmission simulations: attenuation $\alpha = 0.20$ dB/km,

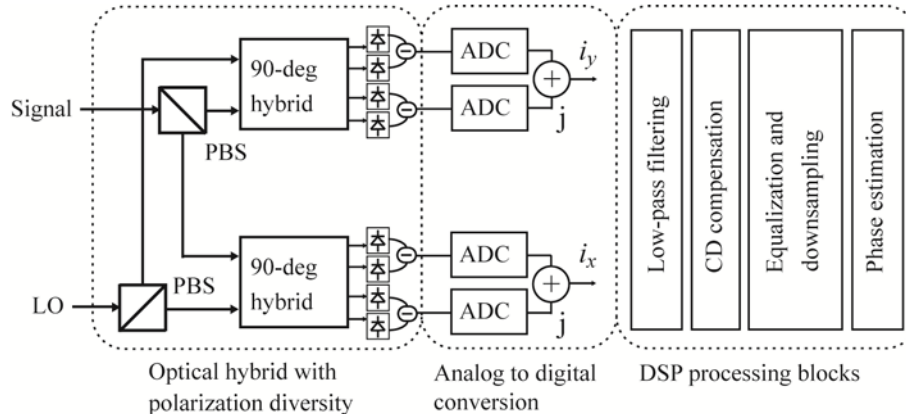


Fig. 4. The coherent receiver used in the simulations.

dispersion coefficient $D = 17$ ps/nm/km, dispersion slope $S = 0.07$ ps/nm²/km, $\gamma = 1.2$ /W/km, and the EDFA noise figure was set to 5.0 dB. Polarization-mode dispersion was not included in our simulations.

3.3 Receiver

The coherent receiver is shown in Fig. 4. The output signals from a 90° optical hybrid with polarization- and phase-diversity are detected by balanced photodetectors and sampled by ADCs at 2 sample per symbol. To model the limited receiver bandwidths, the photocurrents are low-pass filtered (3-dB bandwidth of 0.75 times the symbol rate) with 5th order Bessel filters. CD compensation, if needed, is performed in the frequency domain. The CMA and the DD-LMS algorithms are used to equalize and downsample the signal to 1 sample per symbol. Phase estimation is turned on regardless of whether phase noise is included or not.

3.4 The WDM system

We investigated the performance of two different WDM systems with the same spectral efficiency: *System 1* with fourteen channels at 25 GHz spacing each carrying 112 Gbit/s of data (14 and 16 Gbaud for PM-16-QAM and 128-SP-QAM, respectively), and *System 2* with seven 50 GHz-spaced channels operating at 224 Gbit/s (28 and 32 Gbaud for PM-16-QAM and 128-SP-QAM, respectively). To enable a fair performance comparison, the aggregate data rate was the same for the two systems. In addition, we included the case in which 128-SP-QAM has the same symbol rate as PM-16-QAM, to see how the format performs as a fall-back option. All channels were launched co-polarized, as there is no reason to believe that the launch polarization has a significant influence on the performance. For example, numerical comparisons of PM-QPSK and PS-QPSK have shown that the impact of launch polarization alignment is negligible [12, 19].

Apart from the WDM transmission we included single channel transmission for all data rates, with the motivation that it adds to the understanding of the impact from interchannel WDM crosstalk.

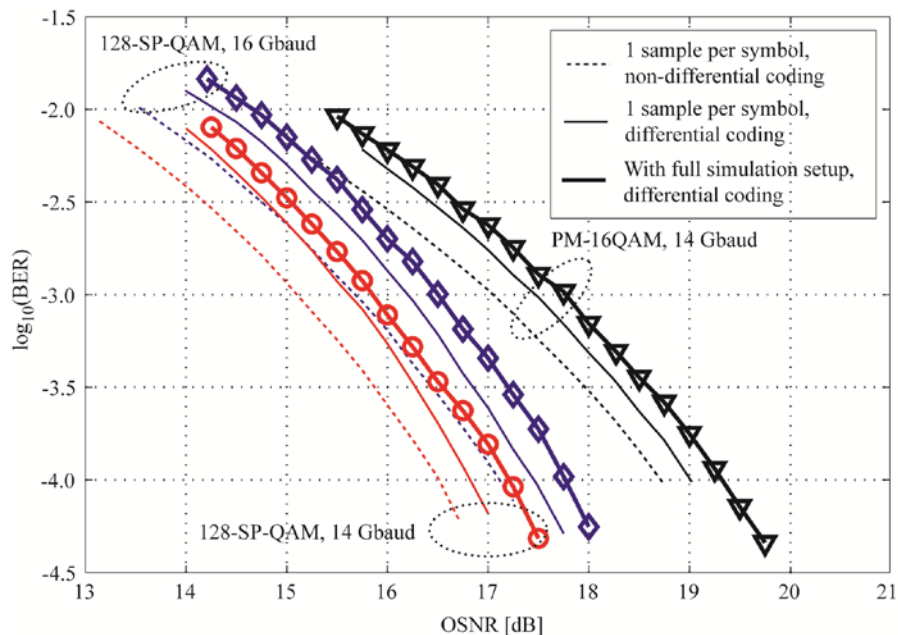


Fig. 5. The BER as a function of the OSNR for 128-SP-QAM at 14 and 16 Gbaud (112 Gbit/s) and for PM-16-QAM at 112 Gbit/s. The thin curves show simulation results for 1 sample per symbol for non-differential coding (dashed lines) and differential coding. The thick lines show the performance when the complete simulation setup is used, including filters.

4. Simulation results

4.1 Back-to-back OSNR

The back-to-back BER as a function of the OSNR is shown in Fig. 5 for PM-16-QAM at 112 Gbit/s, and for 128-SP-QAM at the same bit rate and at the same symbol rate (14 Gbaud). We only show the results for these bit rates since the back-to-back performance at the higher data rates can be found by rescaling the required OSNR. The thin lines show the BER for 1 sample per symbol and without inclusion of the DSP or the filters, meaning that ASE noise is the only impairment. Results are presented for both non-differential (dashed lines) and differential coding (solid lines) of the data. With non-differential coding the difference in required receiver OSNR between the formats at a BER of 10^{-3} is 1.4 dB and 2.0 dB in favor of

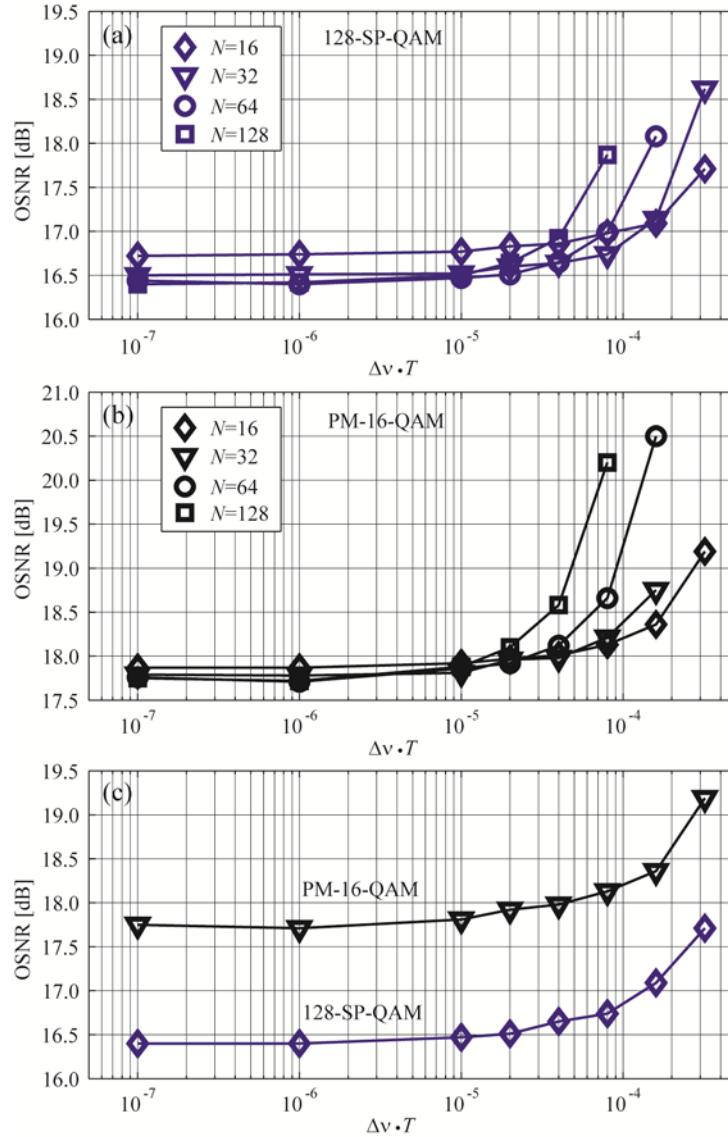


Fig. 6. OSNR required for BER = 10^{-3} as a function of $\Delta\nu \cdot T$ for different block lengths in the phase estimation algorithm for (a) 112 Gbit/s 128-SP-QAM and (b) 112 Gbit/s PM-16-QAM. (c) The required OSNR for the optimal block length for each value of $\Delta\nu \cdot T$.

128-SP-QAM at the same data rate and the same symbol rate as PM-16-QAM, respectively. This is in good agreement with the 1.3 dB difference at 112 Gbit/s that was observed in [10]. The penalties for using differential coding are 0.5 dB and 0.4 dB at a receiver BER of 10^{-3} for 128-SP-QAM and PM-16-QAM, respectively. Subsequently, the difference in required OSNR is reduced by only 0.1 dB compared to non-differential coding.

For differential coding, back-to-back results are also shown with the complete simulation setup as described in section 3, including the filters and DSP algorithms. Compared with PM-16-QAM, the required OSNR to achieve a BER of 10^{-3} is reduced by 1.3 dB and 1.9 dB for 128-SP-QAM with the same data rate and the same symbol rate, respectively. As this difference is very close to the one observed without the DSP and the filters, we conclude that the DSP algorithms work equally well for both formats.

4.2 Linewidth tolerance

Figures 6(a)-(b) show the required OSNR to achieve a BER of 10^{-3} as a function of $\Delta\nu\cdot T$ and the block length N in the phase estimation algorithm for 112 Gbit/s 128-SP-QAM and 112 Gbit/s PM-16-QAM, respectively. The formats have similar linewidth tolerance for the investigated block lengths.

Block lengths of 16 and 32 give good phase noise tracking over a wide range of phase noise variances. In Fig. 6(c), the optimal N is used for each value of $\Delta\nu\cdot T$, and both formats have a 0.5 dB OSNR penalty threshold, compared to the low phase noise regime, at $\Delta\nu\cdot T \approx 10^{-4}$, corresponding to a combined laser linewidth of 1.6 MHz and 1.4 MHz for 112 Gbit/s 128-SP-QAM and PM-16-QAM, respectively. This result is similar to what was achieved in [15] for PM-16-QAM for the same OSNR penalty.

4.3 Transmission performance

Figure 7 shows the BER as a function of the transmission distance for 128-SP-QAM and PM-16-QAM in the two different systems and for both single channel and WDM transmission. The legend shown in Table 1 is used and for all the plots the optimal SSMF launch power has been used.

Figures 7(a)-(b) show the transmission distance when the span length is 60 km for system 1 and system 2, respectively, while Figs. 7(c)-(d) and Figs. 7(e)-(f) show the performance for span lengths of 80 km and 100 km. There is not much to gain in transmission distance by reducing the symbol rate of 128-SP-QAM from 16 to 14 Gbaud or from 32 to 28 Gbaud, only a few percent increase can be expected for both the single channel case and for the WDM case. For both 128-SP-QAM and PM-16-QAM, a doubling of the data rate gives in the single channel case a decrease in reach of about 10-15% for a receiver BER of 10^{-3} . However, in WDM transmission the reach is similar for the two different systems. This is in good agreement with the results presented in [20], in which three different WDM systems using PM-QPSK at different data rates per channel but the same aggregate data rates were compared. The explanation for the behavior is that the relative impact from interchannel nonlinear effects decreases when the symbol rate is increased.

A comparison between PM-16-QAM and 128-SP-QAM at the same data rate reveals a significant advantage in transmission reach at a receiver BER of 10^{-3} for all span lengths for the latter format. For both single channel and WDM transmission, 128-SP-QAM can be transmitted 40-50% longer at both 112 Gbit/s and 224 Gbit/s. This shows that 128-SP-QAM achieves increased reach compared to PM-16-QAM and increased spectral efficiency compared to PM-QPSK. The increase in symbol rate of 14% to maintain a constant data rate is not as substantial as the 33% increase required to use PS-QPSK instead of PM-QPSK [6]. Alternatively, this 14% increase in symbol rate can be used to implement a more advanced FEC code for PM-16-QAM. However, this leads to significantly increased computational complexity which may not be possible to implement at the present time.

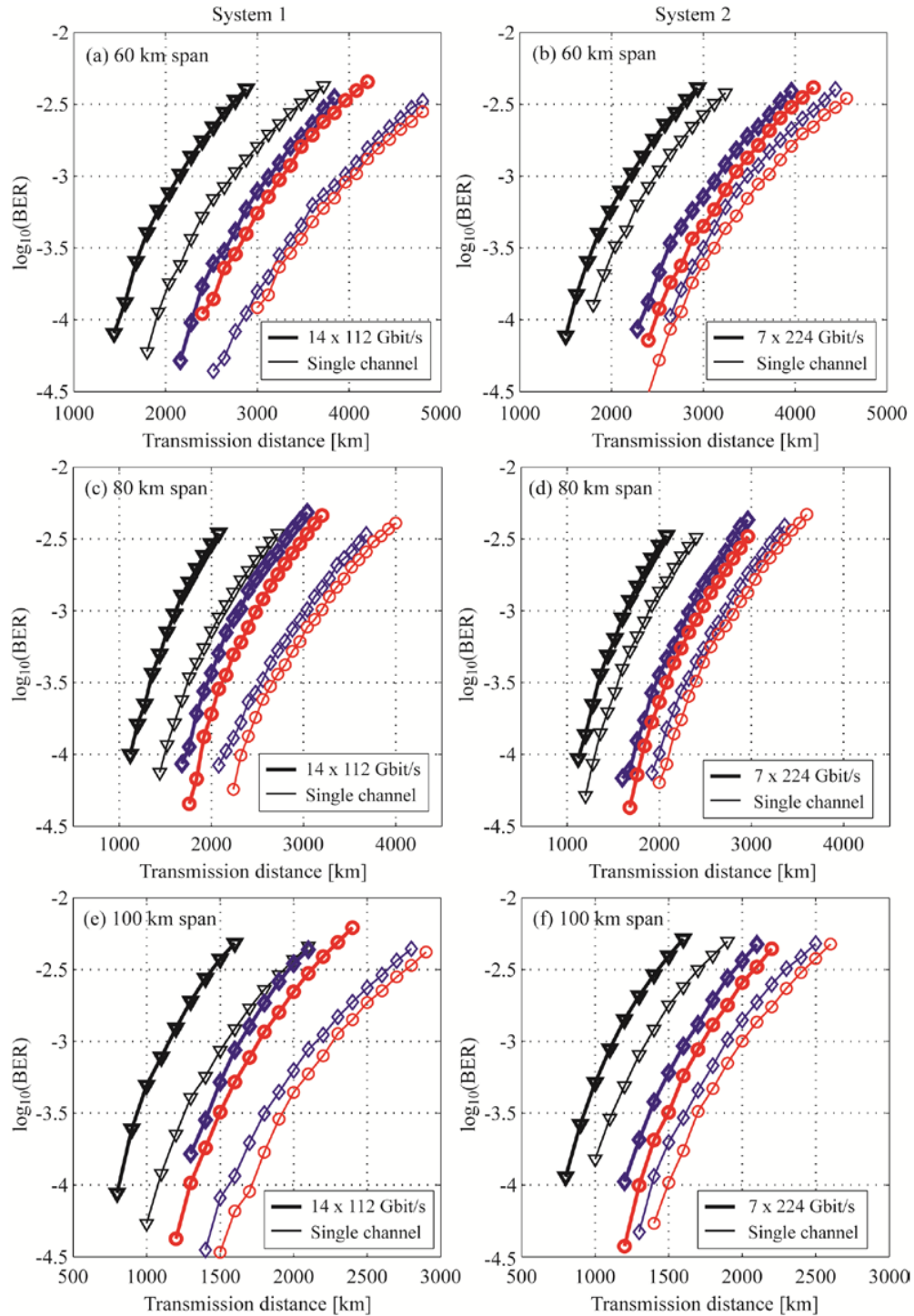


Fig. 7. Transmission distance for different span lengths and data rates for the two different systems. Both the single channel case and the WDM case are shown. (a) 60 km span length, 112 Gbit/s. (b) 60 km span length, 224 Gbit/s. (c) 80 km span length, 112 Gbit/s. (d) 80 km span length, 224 Gbit/s. (e) 100 km span length, 112 Gbit/s. (f) 100 km span length, 224 Gbit/s.

Table 1. Figure Legend for Fig. 7

128-SP-QAM, 16 and 32 Gbaud	
128-SP-QAM, 14 and 28 Gbaud	
PM-16-QAM, 14 and 28 Gbaud	

5. Conclusion

We have performed a numerical comparison of 128-SP-QAM and PM-16-QAM for both single channel transmission and for two different WDM systems with 25 GHz and 50 GHz channel spacing and the same aggregate data rate and spectral efficiency. We have also investigated differential coding for 128-SP-QAM, which avoids error bursts due to cycle slips in the phase noise tracking after coherent detection. Using differential coding for both formats, we found that 128-SP-QAM required 1.3 dB and 1.9 dB lower OSNR than PM-16-QAM at the same bit rate and the same symbol rate, respectively. The penalty from differential coding at a BER of 10^{-3} was 0.5 dB for 128-SP-QAM, compared to 0.4 dB for PM-16-QAM. We performed simulations including laser phase noise and found the phase noise tolerance to be similar for the two formats for the algorithms that we used. The algorithms also turned out to perform equally well for 128-SP-QAM and PM-16-QAM.

In the transmission simulations, 128-SP-QAM at the same data rate as PM-16-QAM achieved 40-50% longer transmission reach at a receiver BER of 10^{-3} for all investigated span lengths and for both single channel and WDM transmission. Furthermore, our results show that the transmission reach in the two WDM systems is similar, although the data rate per channel is two times higher in system 2.

Acknowledgment

We acknowledge the financial support from the Swedish foundation for strategic research (SSF).